Optimization of tunnels excavation sequences in Egyptian soil conditions

Ahmed T. Abd Ellaah*, Mohamed A. Eid**, Mostafa Z. Abd Elrehim** and Waleed Abdullah***

* *Kuwait Building House Company, Civil Engineering Department, Kuwait.*

** *Minia University, Civil Engineering Department, Minia, Egypt.*

*** *Kuwait University. Civil Engineering Department, Kuwait.*

* *Corresponding author: ATA20050@yahoo.com*

Submitted: 30-01-2022

Revised: 28-04-2022

Accepted: 07-05-2022

ABSTRACT

Construction of huge metro projects in congested areas in Cairo City, Egypt, calls for optimization of the underground excavation process. The soil profile in Cairo city, Egypt, is generally characterized as soft soil containing layers of clay and sand. To control the ground movements and shotcrete stresses, it is necessary to optimize the ground surface settlements and excavation step. In this paper, several tunnel sections were compared to illustrate how the tunnel shape affects the soil deformations and straining actions results. Results of numerical modeling using plane-strain finite elements are presented; different types of sequences for the tunneling excavation of each section are compared. Analysis results from different models show that using different tunnel section excavation sequences affects the soil behavior differently, and that suitability of the sequence is determined by the soil properties and the dimensions of the tunneling section.

Keywords: Underground excavation; Sequences; Tunnels; Soft soil.

INTRODUCTION

Nowadays, there are many construction methods for underground structures (tunnels & stations) such as machine methods, New Austrian Tunneling Method (NATM) and Cut-Cover method. Cairo metro Line 1 was constructed using Cut and Cover Method. For Lines 2 and 3, the tunnels were constructed using Tunneling Boring Machine (TBM) (NAT, 2009). Since underground structures are usually built in congested areas, major problems generally occur at construction stages. For cases that include large underground openings, successful measures that include pre-supporting systems are employed to enhance ground stability and reduce ground surface settlement (Mostafa Z., Ahmed T., 2016).

Section excavation causes stress redistribution, which induces movements in soil media and ground surface (Sauer, 1990). Therefore, it is crucial to assure ground stability during excavation sequences and maintain control over the expected deformations and its effects on nearby structures. In congested urban zones, the effect of underground construction on nearby structures is an important factor since it causes volume losses which are reflected on the surface creating ground movements that can affect the existing nearby structures. Soil movements are estimated in the early stages of designing and planning tunnel excavations using empirical, analytical or numerical methods. However, the interaction between underground works, substructures linings and super structures during the construction of underground structures is a highly complex phenomenon, which may cause the surrounding ground to behave unexpectedly. There are no other studies that particularly focus on the ground surface settlements and excavation steps for optimization. Therefore, this study is aimed at using numerical modeling to better understand the behavior of the soil during the construction of underground structures and to predict the expected effects on nearby structures.

NEW AUSTRIAN TUNNELING METHOD (NATM)

New Austrian Tunneling Method (NATM), also referred to as the old Austrian tunneling method, was developed in Austria between 1957 to 1965. NATM could also be called as sprayed concrete lining (SCL) or sequential excavation method (SEM) (Alun, 2019). It is one of the most popular methods of tunnel design and constructions. Rabcewicz (1964), the principal founder of NATM, described its basic structure to consist of thin sprayed concrete linings, where each lining resembles a complete ring with an "auxiliary arch" piece; the deformation in the arch is measured as a function of time until equilibrium is obtained. This mechanism was summarized in three points by Karakus and Fowell (2003) and Karakus, Fowell (2004) as follows:

1. Application of a thin-sprayed concrete lining.
2. Closure of the ring as soon as possible.
3. Systematic deformation measurement.

NATM is more economically advantageous than other methods because, in NATM, the geological stresses of the surrounding soil mass can also be used to provide stabilization and support to the tunnel itself. Arshad and Abdullah, (2016) emphasized the importance of controlling and predicting the phenomenon of ground surface settlements that occur during and after the tunnel excavations that may cause damages to the nearby structures.

CONSTRUCTION SEQUENCES

Typical excavation sequences usually involve excavation followed by supporting a part of the tunnel section using initial shotcrete, followed by excavating and supporting other parts using shotcrete and finally activating the final lining of the tunnel. The ground movements are controlled by optimizing the construction procedure and excavation steps, which have an effective influence (Mahdi M., Shariatmadari N. 2014). To control the soil deformation and maintain excavation stability, excavation sections are divided into small parts. The number of excavation parts for the section and its excavation arrangement mainly depends on the soil properties and environmental requirements, especially in urban areas where less deformation is required (FHWA, 2009). The most popular excavation sequences in soft ground are shown in Figure (1).

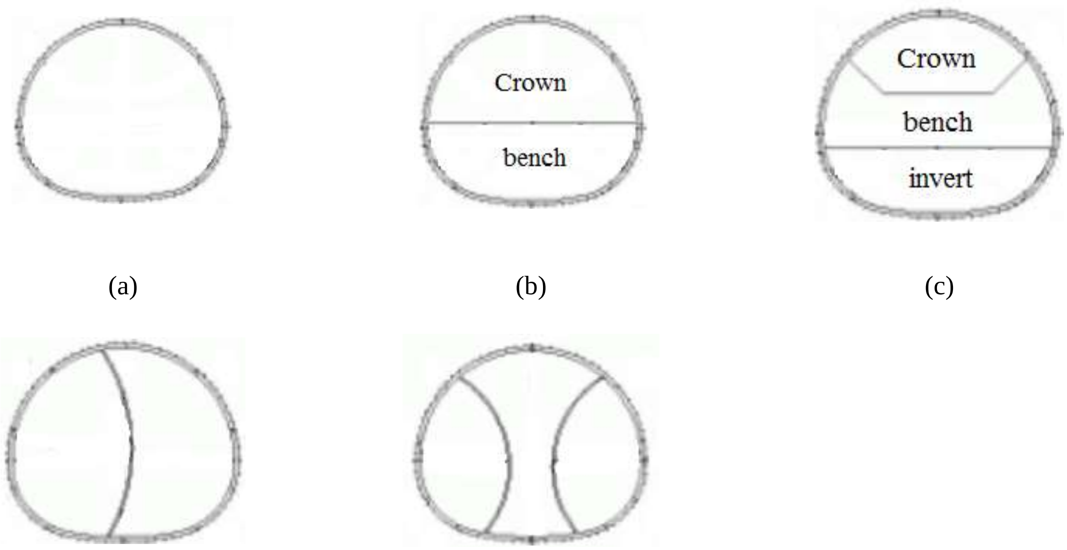

Figure 1. Most popular NATM excavation sequences in soft ground

NUMERICAL MODELLING OF CONSTRUCTION SEQENCES OF NATM SECTIONS

Vydrova (2015) showed that dividing the tunnel face into a higher number of partial sequences may cause negative effects. In this study typical soil profiles along the metro lines in Cairo, Egypt, which is generally characterized as soft soil with layers of clay and sand, were investigated (Shata, (1988) and Said, (1962)). Three tunnel excavation cross sections with the corresponding construction sequences were selected to be modeled, analyzed and compared together to determine the optimum cross section and construction sequence that minimize deformations to within allowable limits herein. The three different cross sections are described below.

The first illustration is a circular shape with a diameter of 6.0 m, as shown in Figure (2.a). The construction sequences that were observed for the for the first shape (group one) are shown in Figure (3.a, b, c, d, e, f, g, h, i, j and k). The second shape is a section with dimensions, as shown in Figure (2.b) and it represents the section that has a smaller width compared to its height. The observed construction sequences for the second shape (group two) are shown in Figure (4.a,b,c,d,e,f,g,h,i,j and k). Third shape is a section with dimensions, as shown in Figure (2.c) and it represents the section that has a larger width compared to its height. Studied construction sequences for the third shape (group three) are shown in Figure (5.a,b,c,d,e,f,g,h,i,j and k).

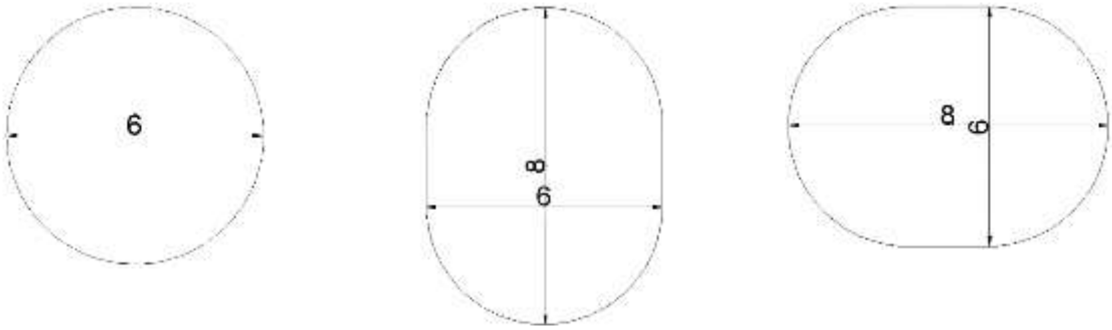

(a) Group One (b) Group Two (c) Group Three

Figure 2. Dimensions of sections of the models (in meter)

Excavation and construction sequences for the cross section shown in Figures 3, 4, and 5 are described below. For models with more than one sequence, construction starts with sequence 1.

a) Full excavation (Model 0).

b) Crown and bench excavation (Model 1).

c) Crown, bench and invert excavation (Model 2).

d) Single side wall drift excavation (Model 3).

e) Single side wall drift excavation (Model 4): left crown and left bench.

f) Single side wall drift excavation (Model 5): left crown, left bench, then right crown and right bench.

g) Double side wall drift excavation (Model 6).

h) Double side wall drift excavation (Model 7): left crown, left bench, right crown, right bench middle crown, and middle bench.

i) Double side wall drift excavation (Model 8): left crown, left bench, right crown, right bench, middle crown, middle bench, and middle invert.

j) Double side wall drift excavation (Model 9): left crown, left bench, left invert, right crown, right bench, right invert, middle crown, and middle bench.

k) Double side wall drift excavation (Model 10): left crown, left bench, left invert, right crown, right bench, right invert, middle crown, middle bench, and middle invert.

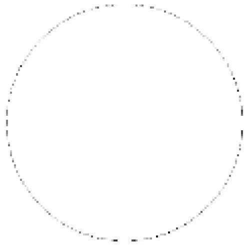

(a) Section used in Model 0

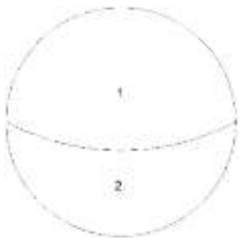

(b) Section used in Model 1

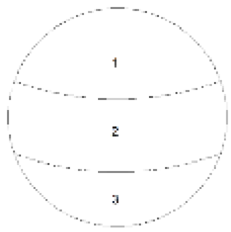

(c) Section used in Model 2

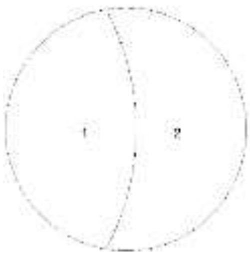

(d) Section used in Model 3

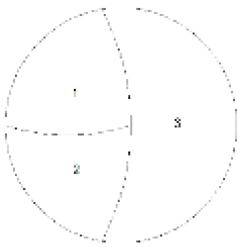

(e) Section used in Model 4

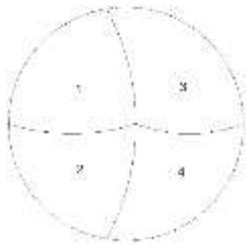

(f) Section used in Model 5

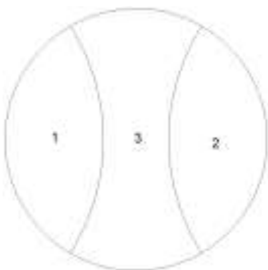

(g) Section used in Model 6

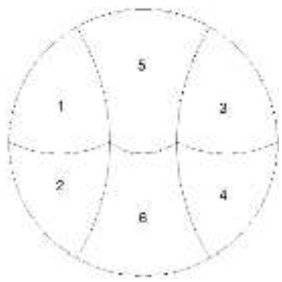

(h) Section used in Model 7

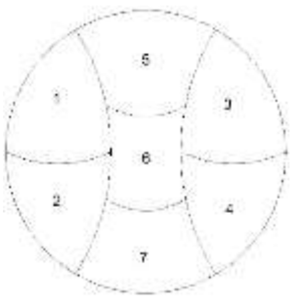

(i) Section used in Model 8

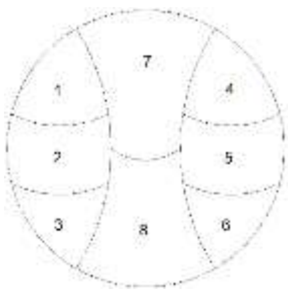

(j) Section used in Model 9

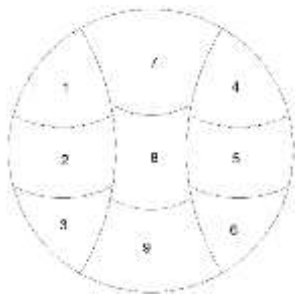

(k) Section used in Model 10

Figure 3. Observed construction sequences in group one

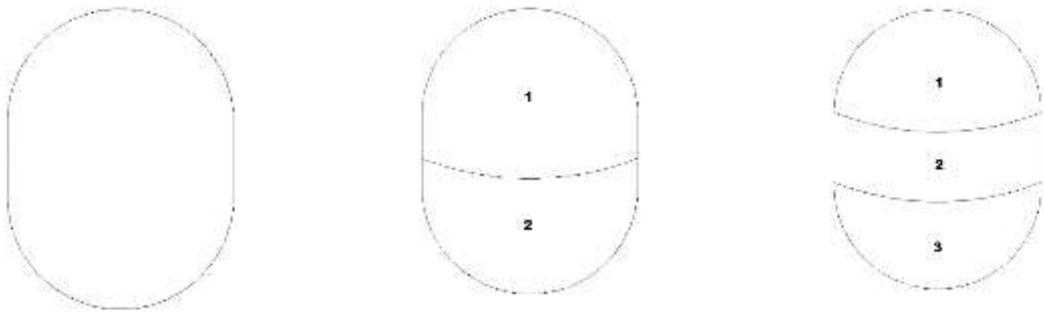

(a) Section used in Model 0 (b) Section used in Model 1 (c) Section used in Model 2

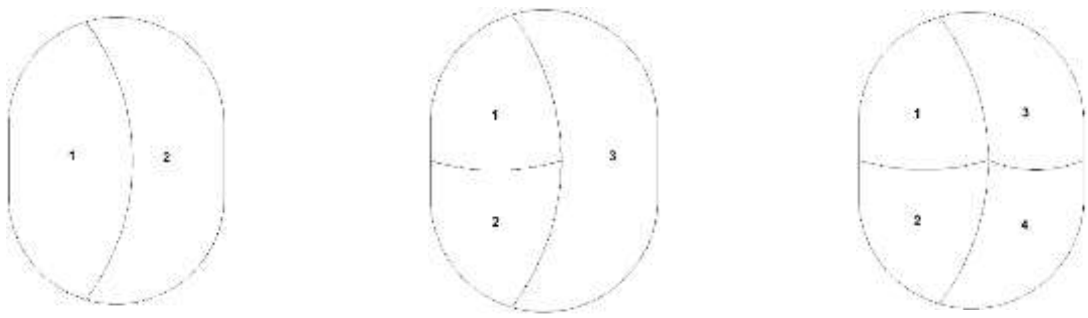

(d) Section used in Model 3 (e) Section used in Model 4 (f) Section used in Model 5

(g) Section used in Model 6 (h) Section used in Model 7

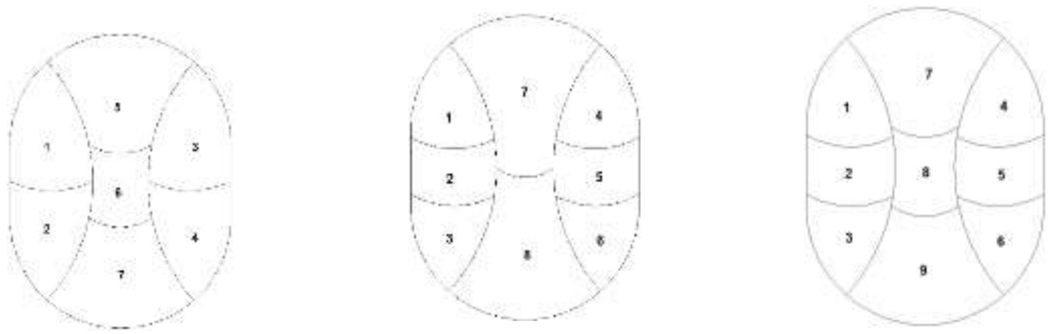

(i) Section used in Model 8 (j) Section used in Model 9 (k) Section used in Model 10

Figure 4. Observed construction sequences in group two

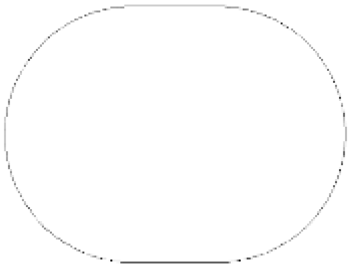

(a) Section used in Model 0

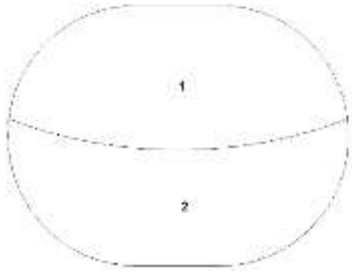

(b) Section used in Model 1

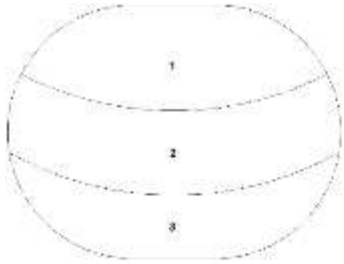

(c) Section used in Model 2

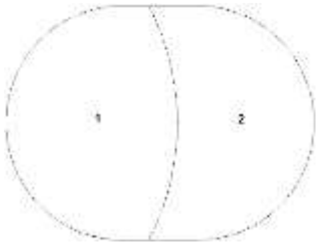

(d) Section used in Model 3

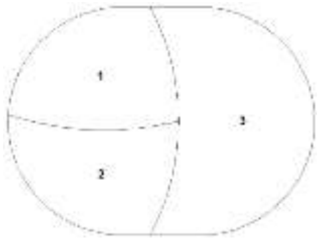

(e) Section used in Model 4

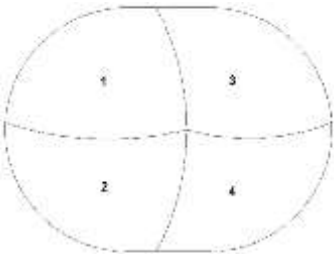

(f) Section used in Model 5

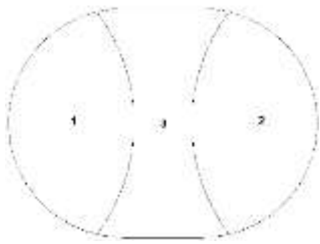

(g) Section used in Model 6

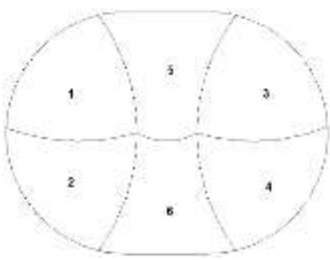

(h) Section used in Model 7

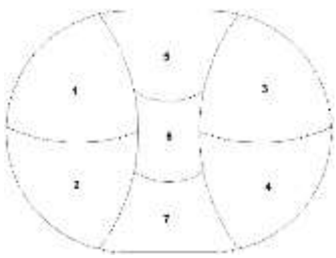

(i) Section used in Model 8

(j) Section used in Model 9 (k) Section used in Model 10

Figure 5. Observed construction sequences in group three

Material and construction sequence simulation in numerical models

Material modeling was done in Finite Element program, Midas package (MIDAS, MIDAS GTS NX V3.0.0(4)). The soil media was modeled using a six node linearly varying strain triangular finite elements (L.S.T). The shotcrete lining was modeled using beam elements. Mohr-Coulomb's non-linear material failure model was used for soil description and elastic linear behavior was adopted for modelling concrete elements. Meshes with sufficient depth and width were used to model the soil infinite conditions. The boundary conditions were modeled to restrict the vertical and horizontal movements at the bottom of the model while horizontal movements were restricted at both sides. The excavation process is simulated in steps (Eid and Zaki AbdElrehim, 2013). To prevent any unbalanced load force caused by continuous excavation the load is distributed using the Load Distribution Factor (LDF). The excavated part is removed, followed by the installation of a temporary lining and stress elimination of the excavated soil. The tunnel is constructed in the soil at a depth of 15 m in the absence of ground water. Model is made of two layers, as shown in Figure (6). The top layer is a fill layer, followed by a sand or a clay layer. Surface loads of 18 kN/m^2 are considered for the model (NAT, 2011).

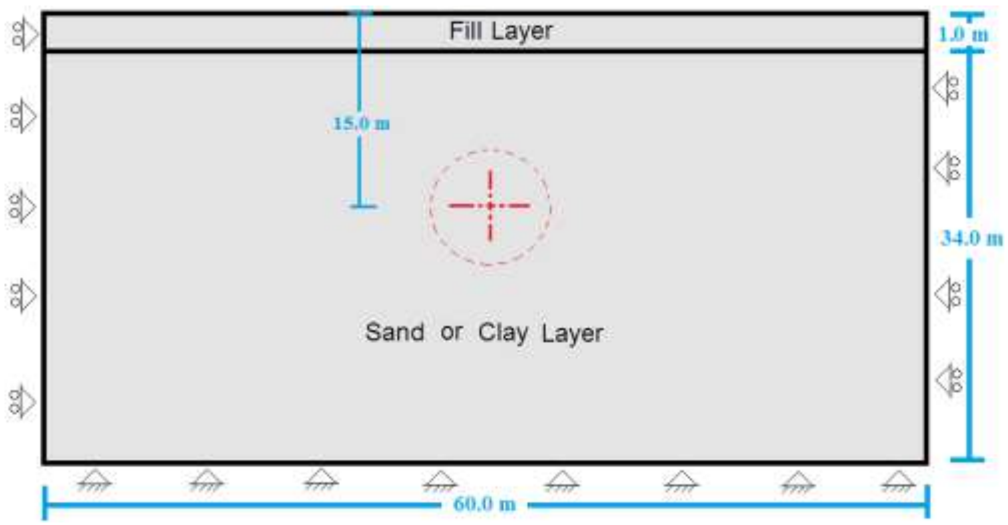

Figure 6. Finite element model showing soil layers and tunnel details

Table 1. Properties of the soil layers used in the models

Soil Layer	Modulus of Elasticity	Poisson's Ratio	Unit Weight	Cohesion	Friction Angle	Lateral Pressure Factor
	E	υ	γ	c	Ø	K_0

	kN/m²		**kN/m³**	**kN/m²**	**degree**	
Fill	10000	0.45	18.00	-	30	0.48
Sand	75000	0.30	19.50	-	38	0.50
Clay	60000	0.45	20.00	200.00	-	0.33

Table 2. Properties of the concrete elements used in different models

Concrete Element	Modulus of Elasticity E kN/m²	Poisson's Ratio υ	Weight Density γ kN/m³	Thickness m
Shotcrete	15000000	0.20	25	0.20
Final Lining	32000000	0.20	25	0.40

RESULTS

The main results of the investigation show the induced deformations in the surrounding soil and at ground surface. Results are presented in terms of the measured settlement values that occur at surface and tunnel crown during the construction stages in both sandy and clayey soil types. Then, these values are compared with "Model 0" results and presented in terms of percentages. Critical plastic point zones are also presented to check the ground stability during construction.

A. **Results for group one: circular tunnel with 6.0 m diameter**

Sandy soil

Analysis results of this group are shown in Figures (7), (8) and (9), wherein the surface settlement profiles, relative settlement (%) compared to Model (0), and critical plastic zones, respectively, are presented. Graphs from Figure (7) show that "Model 0" produces the highest surface settlement value. Although "Model 1" does not produce a better value than "Model 0" in terms of surface settlement, it produces comparatively fewer plastic points. Surface settlement values produced by other models are less than 60 % of that produced in "Model 0". From the chart depicted in Figure (8), "Model 1" produces crown settlement of 88% of the crown settlement in "Model 0". The crown settlement values produced by other models lie in the range between 57 and 67% of the crown settlement value produced in "Model 0". Although "Model 3" produces small displacements values, the plastic point has wide existence and distribution, as shown in Figure (9).

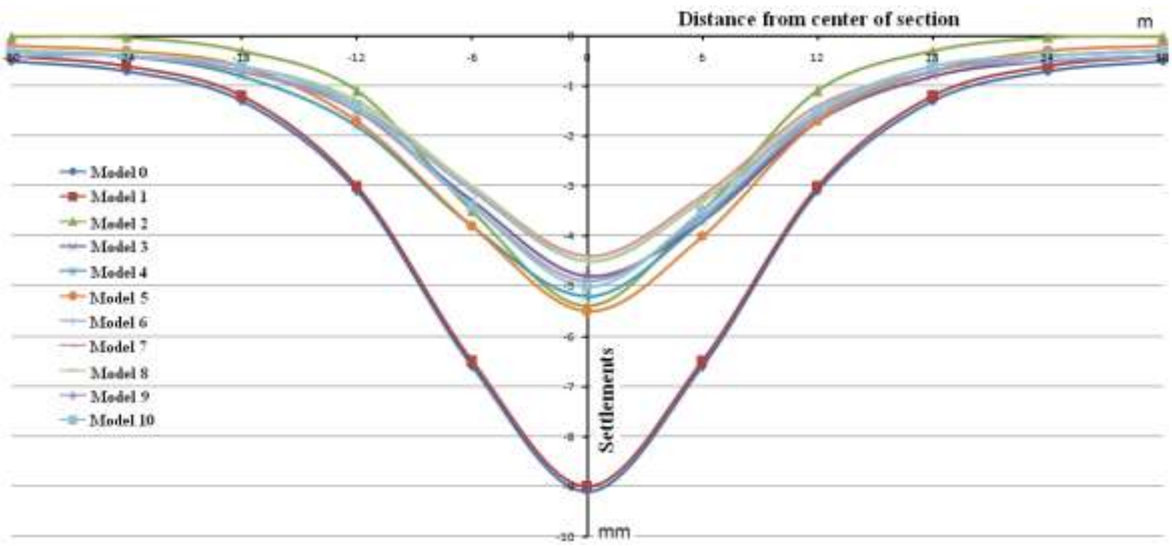

Figure 7. Surface settlements in sandy soil (Group one)

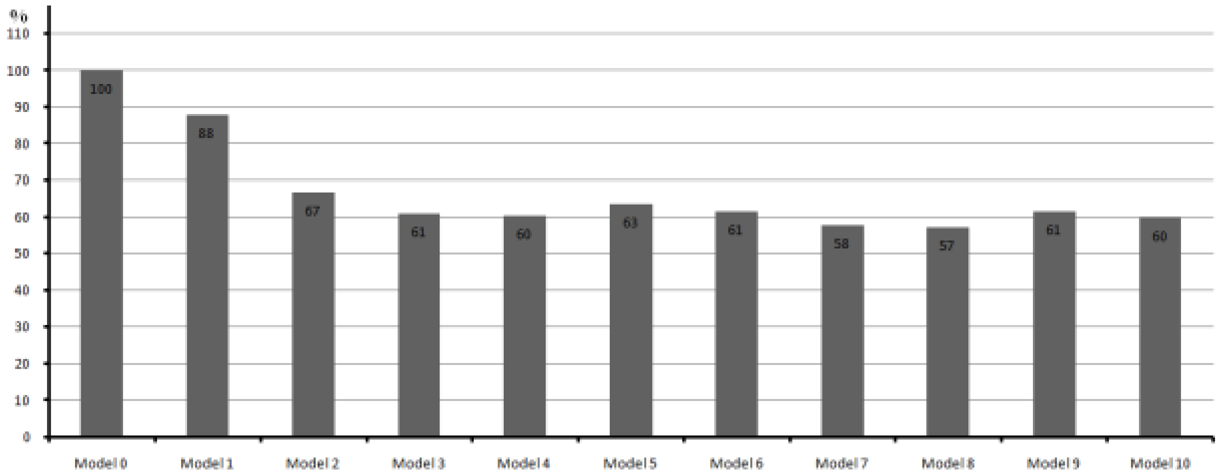

Figure 8. Percentage of the crown settlement in sandy soil compared to Model (0) (Group one)

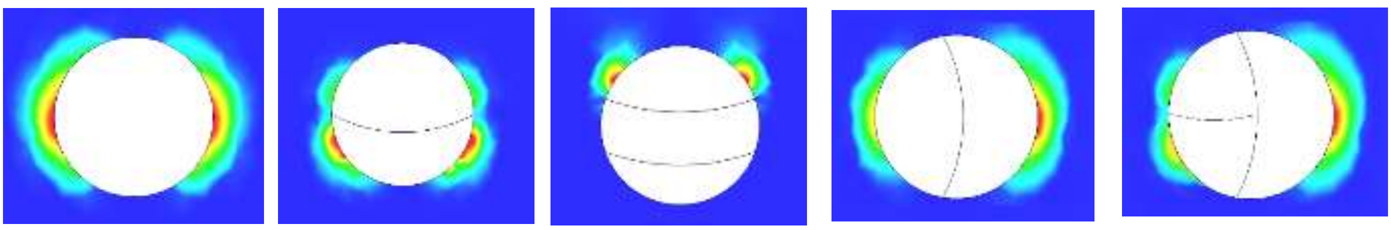

(a) in "Model 0" (b) in "Model 1" (c) in "Model 2" (d) in "Model 3" (e) in "Model 4"

Figure 9. Plastic points zone in sandy soil (Group one)

Clayey soil

Analysis results of this group are shown in Figures (10), (11) and (12). Results in Figure (10) show that "Model 0" and "Model 1" produce the highest surface settlement value. In terms of surface settlement, "Model 1" does not produce better results than "Model 0"; however, it produces comparatively fewer plastic points, as shown in Figure (12). Other models produce surface settlement values of less than 80 % of that produced in "Model 0". From the chart shown in Figure (11), "Model 2" produces 82% crown settlement of that in "Model 0". Other Models produce crown settlement ranging between 67 and 73% of crown settlement produced in "Model 0".

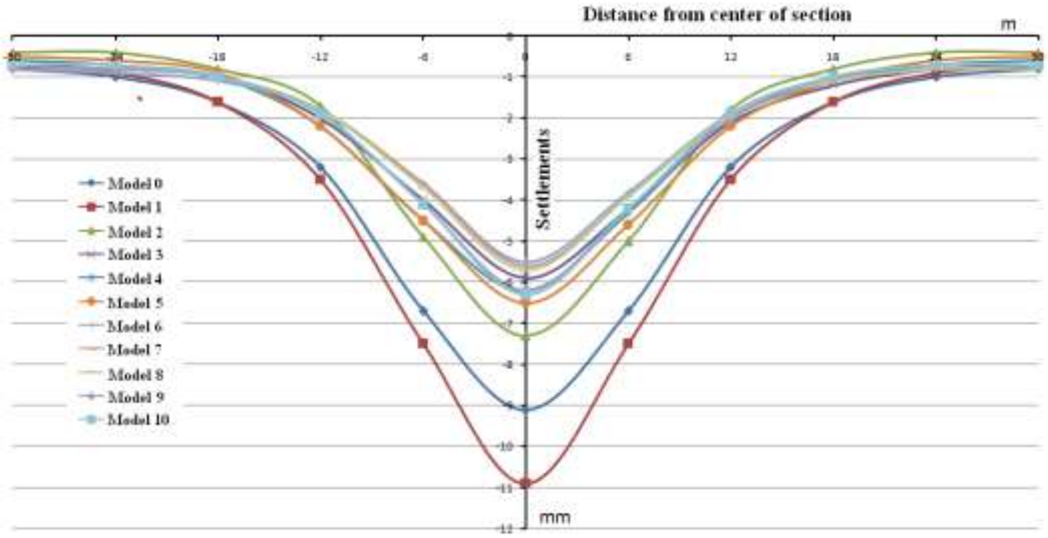

Figure 10. Surface settlements in clayey soil (Group one)

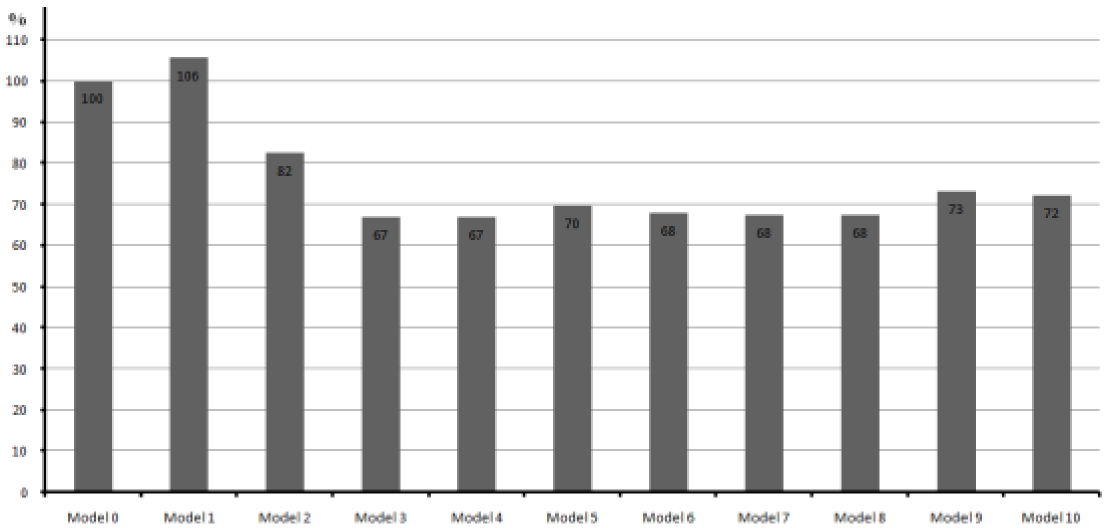

Figure 11. Percentage of crown settlement in clayey soil compared to that in Model (0) (Group one)

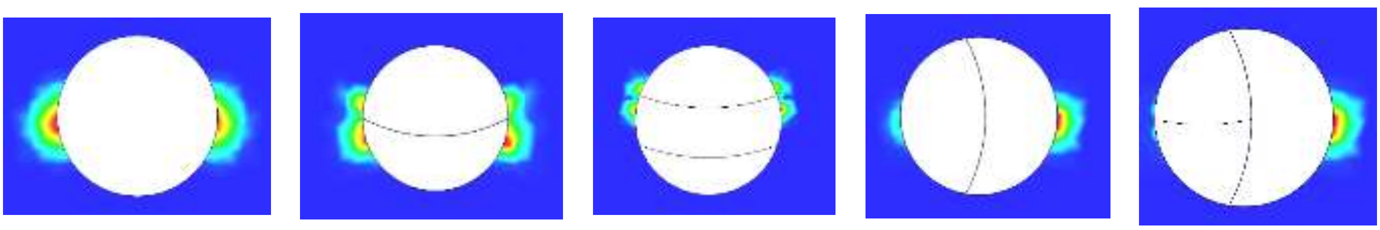

(a) in "Model 0" (b) in "Model 1" (c) in "Model 2" (d) in "Model 3" (e) in "Model 4"

Figure 12. Plastic points zone in clayey soil (Group one)

B. Results for group two: tunnel with section that has width smaller than its height

Sandy soil

Analysis results of this group are shown in Figures (13), (14), and (15). Figure (13) results show that "Model 0" produces the highest surface settlement value. Other models produce less than 75% surface settlement values of that produced in "Model 0". From the chart in Figure (15), the crown settlement values produced by models lie in the range between 44 and 73% of that produced in "Model 0". Although "Model 3" produces small displacements values, the plastic point has wide existence and distribution as shown in Figure (15).

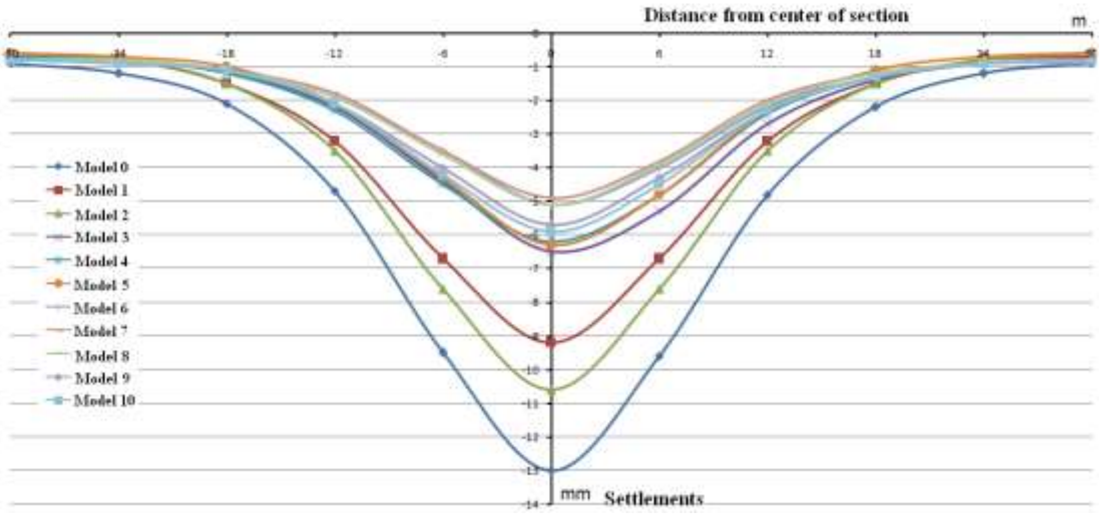

Figure 13. Surface settlements in sandy soil (Group two)

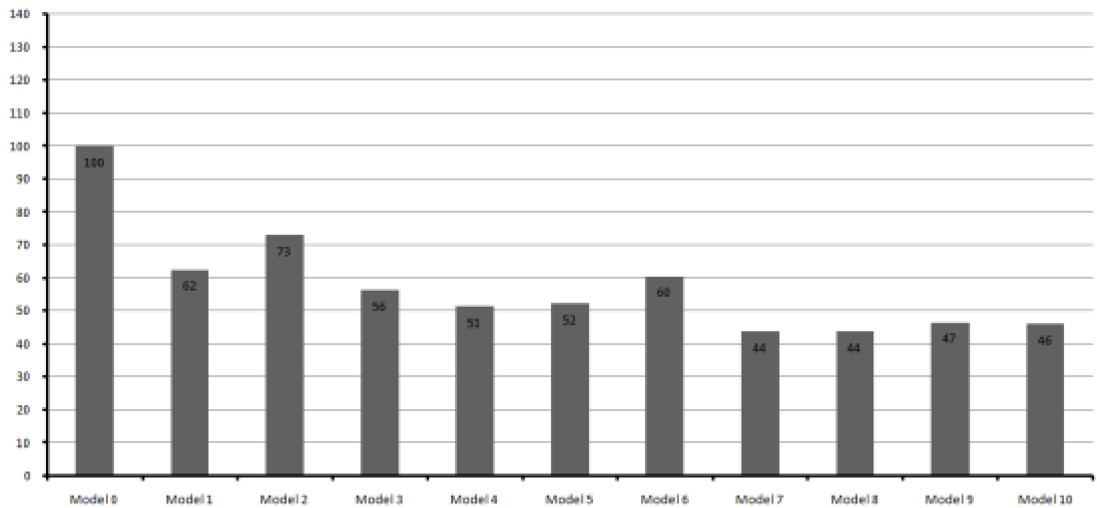

Figure 14. Percentage of settlement at crown in sandy soil compared to Model (0) (Group two)

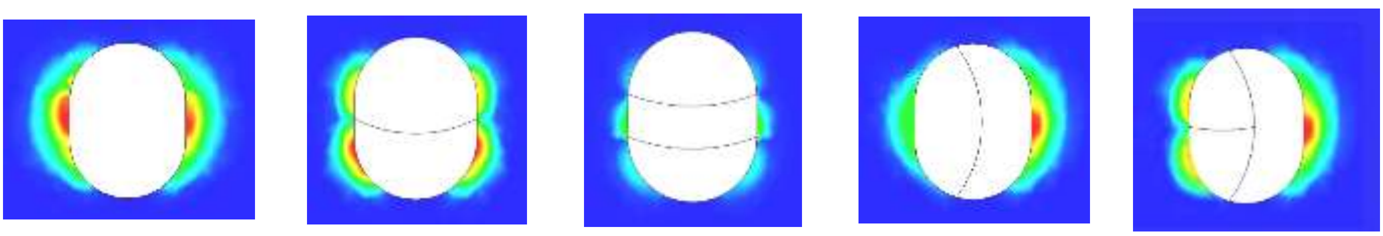

(a) in "Model 0" (b) in "Model 1" (c) in "Model 2" (d) in "Model 3" (e) in "Model 4"

Figure 15. Plastic points zone in sandy soil (Group two)

Clayey soil

Analysis results of this group are shown in Figures (16), (17), and (18). From the results in Figure (16), "Model 0", "Model 1" and "Model 2" produce the highest surface settlement values. Although "Model 1" and "Model 2" do not produce better values than "Model 0", in terms of surface settlement, they produces fewer plastic points as shown in Figure (18). Other models produce surface settlement values less than 80 % of that produced in "Model 0". From the chart in Figure (17), the crown settlement values produced by the models lie in the range between 69 and 78% of crown settlement produced in "Model 0".

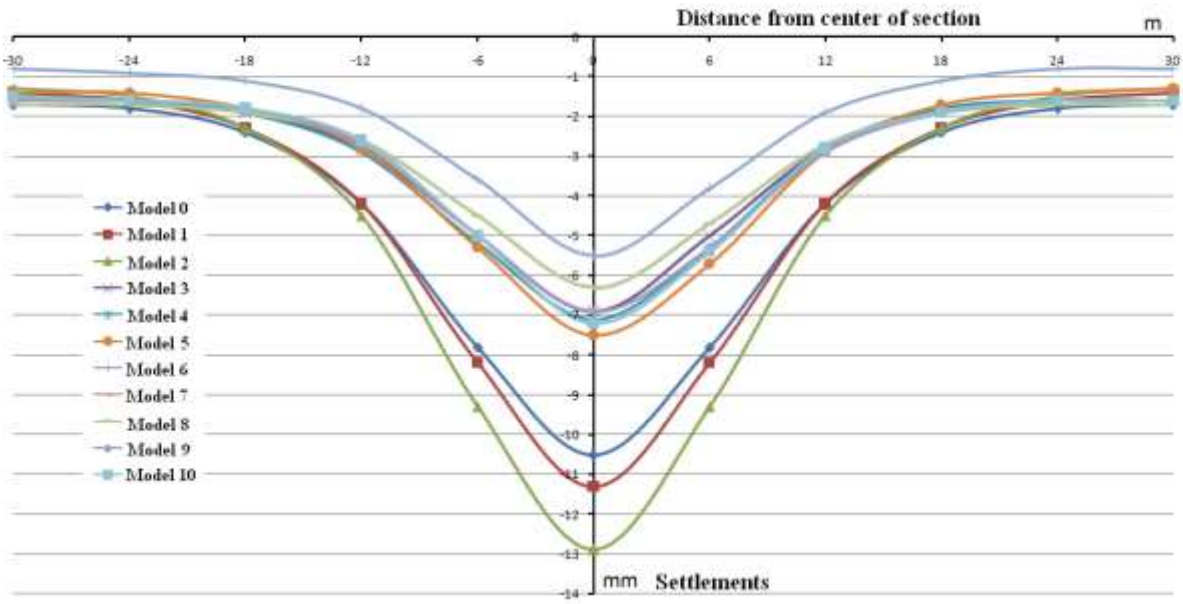

Figure 16. Surface settlements in clayey soil (Group two)

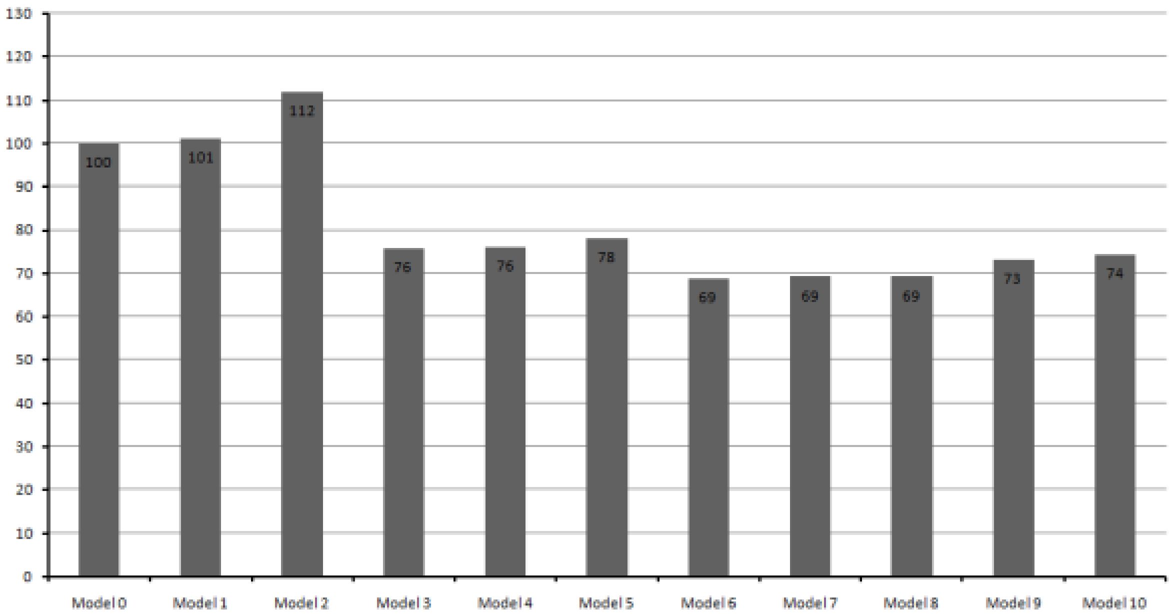

Figure 17. Percentage of crown settlement values in clayey soil compared to Model (0) (Group two)

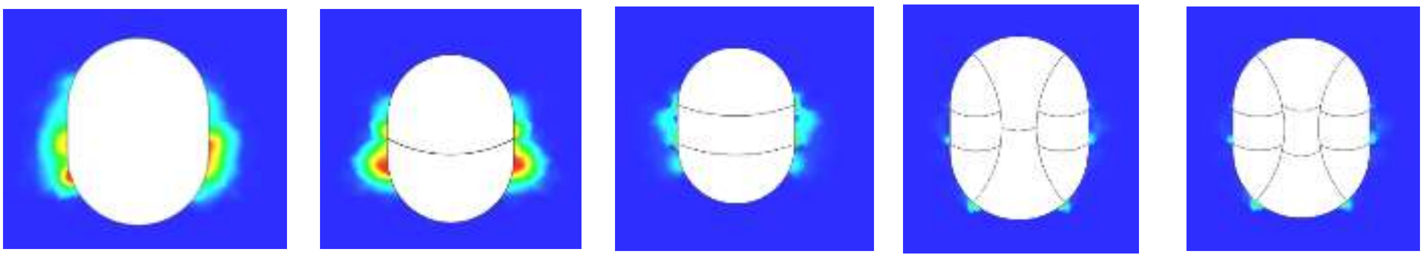

(a) in "Model 0" (b) in "Model 1" (c) in "Model 2" (d) in "Model 9" (e) in "Model 10"

Figure 18. Plastic points zone in clayey soil (Group two)

C. Results for group three: tunnel with section that has width larger than height

Sandy soil

Analysis results of this group are shown in Figures (19), (20), and (21). Results in Figure (19) show that "Model 0", "Model 1" and "Model 2" produce the highest surface settlement values. Although "Model 1" and "Model 2" do not produce better values than "Model 0" in terms of surface settlement, it produces fewer plastic points, as shown in Figure (21). Other models produce surface settlement values less than 80 % of that produced in "Model 0". From the chart in Figure (20), the crown settlement values produced by models lie in the range between 71 and 77% of that in "Model 0".

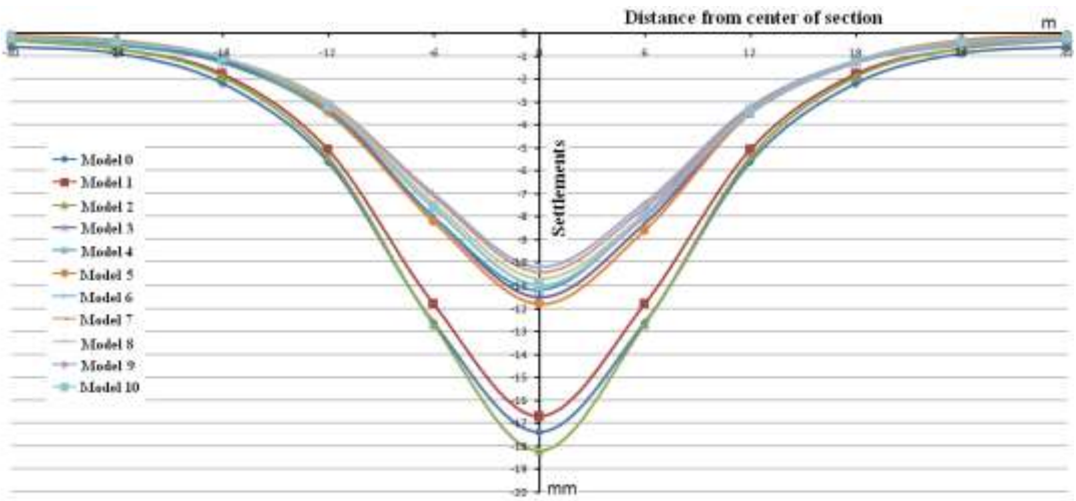

Figure 19. Surface settlements in sandy soil (Group three)

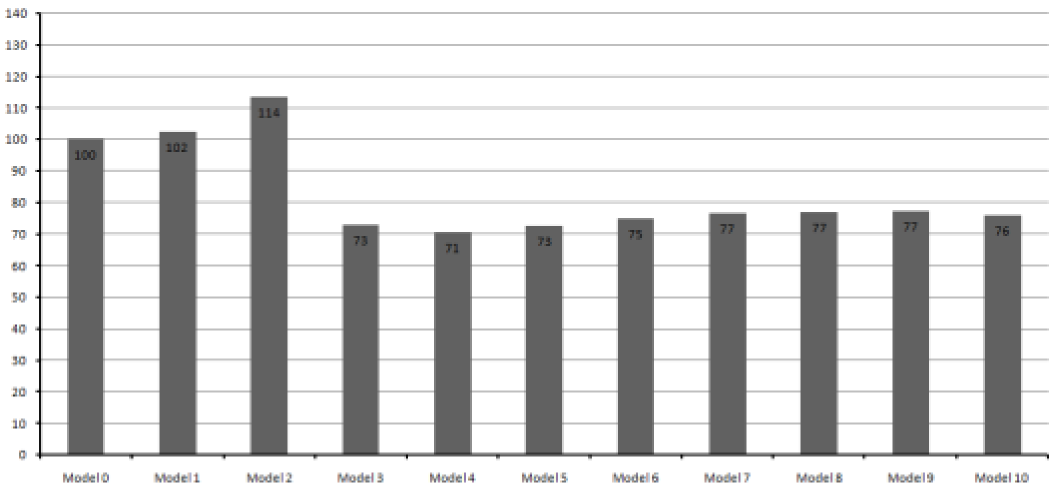

Figure 20. Percentage of crown settlement value in sandy soil compared to Model (0) (Group three)

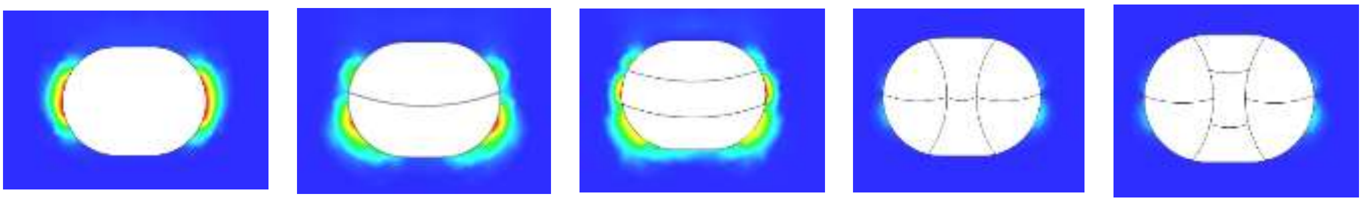

(a) in "Model 0" (b) in "Model 1" (c) in "Model 2" (d) in "Model 7" (e) in "Model 8"

Figure 21. Plastic points zone in sandy soil (Group three)

Clayey layer

Analysis results of this group are shown in charts in Figures (22), (23), and (24). "Model 0", "Model 1", and "Model 2" produce the highest surface settlement value. Although "Model 1" and "Model 2" do not produce better values than "Model 0" in terms of surface settlement, they produces fewer plastic points. Surface settlement values produced by other models are less than 90 % of that produced in "Model 0". From the chart in Figure (23), the crown settlement values produced by models lie in the range between 66 and 93% of that produced in "Model 0". Plastic point zone disappears in "model 7", as shown in Figure (24).

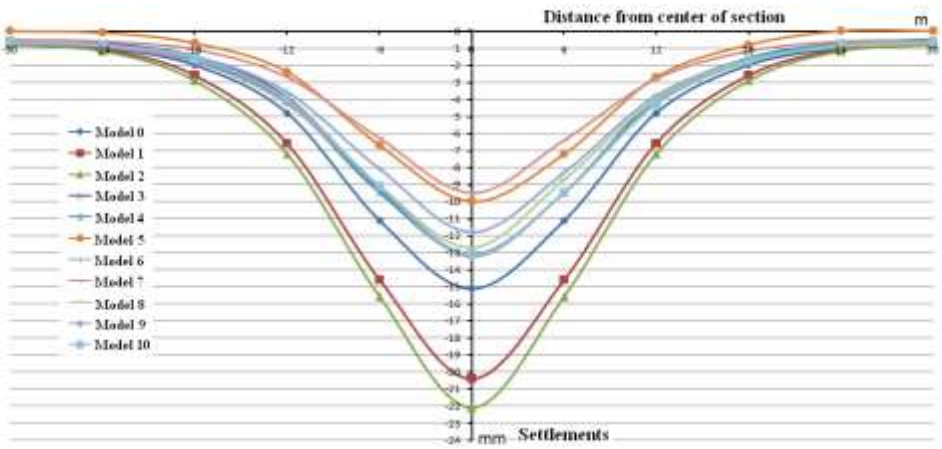

Figure 22. Surface settlements in clayey soil (Group three)

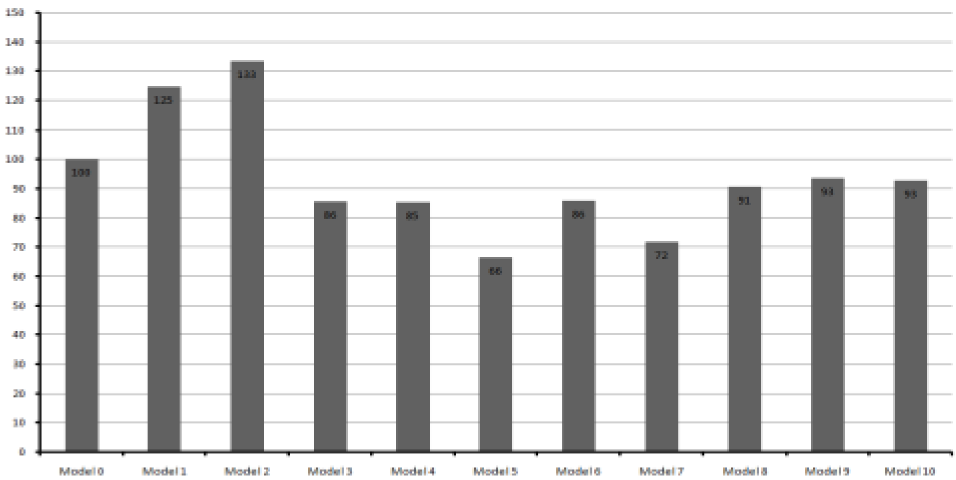

Figure 23. Percentage of crown settlement in clayey soil compared to Model (0) (Group three)

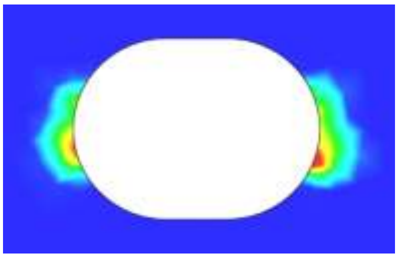

(a) in "Model 0"

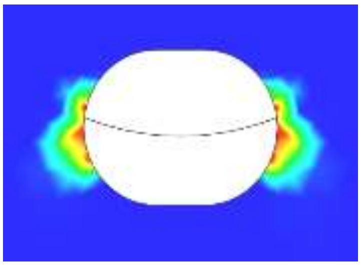

(b) in "Model 1"

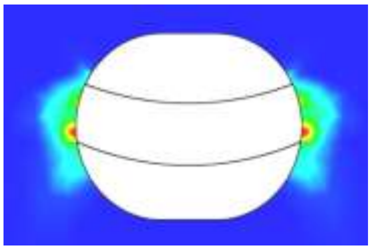

(c) in "Model 2"

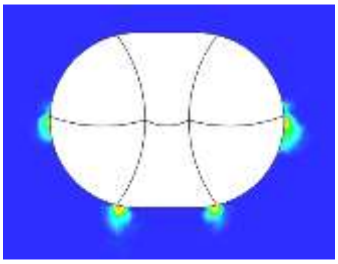

(d) in "Model 7"

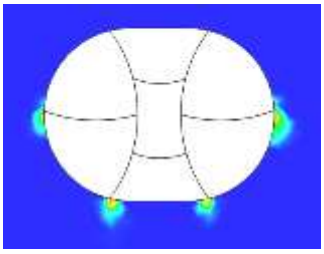

(e) in "Model 8"

Figure 24. Plastic points zone in clayey soil (Group three)

DISCUSSION AND COMMENTS

In case of group one that has a section with equal width and height, the displacements can be reduced using both techniques, that is, crown and bench excavation, and side wall drift excavation. The area of plastic points zone remains large in case of side wall drift excavation technique and decreases significantly in case of crown and bench excavation technique. Whereas, in clay layers, the plastic points zone decreases substantially in the case of side wall drift excavation technique. Therefore, the crown and bench excavations model is preferred in case of group one in sand layers, and the side wall drift excavations model is preferred in clay layer for the same group. In addition, dividing the tunnel section into small parts would allow plastic points and soil deformation to be controlled effectively.

In case of group two that includes a section with width smaller than its height, the displacements can be reduced by both crown and bench excavation and side wall drift excavation techniques for sand layers. In clay layers, the displacements can be reduced efficiently by side wall drift excavation. However, in case of side wall drift excavation technique, plastic points zone remains a large area and it can be reduced efficiently in case of crown and bench excavation technique. Therefore, for sand and clay layers, crown, bench and invert excavations are the preferred techniques. Moreover, dividing the tunnel section into small parts could allow plastic points and soil deformation to be controlled effectively.

In case of group three, which has a section with width larger than height, dividing the tunnel section into small parts enabled to control plastic points and soil deformations. In this case, the displacements can only be reduced using the side wall drift excavation technique. However, the plastic points' zone can be reduced by combining the crown and bench excavation, and side wall drift excavation techniques. In clay layers, the crown and bench excavation can increase the displacement widely because section produced from excavation stages, as shown in Figure (25), is unfavorable. Therefore, side wall drift excavation technique is the preferred in sand and clay layer. In special cases, the construction needs to use crown and bench excavation and side wall drift excavation techniques together to decrease the surface settlements to avoid any damage that may occur to the nearby structures and to avoid any collapse around the section of the tunnel.

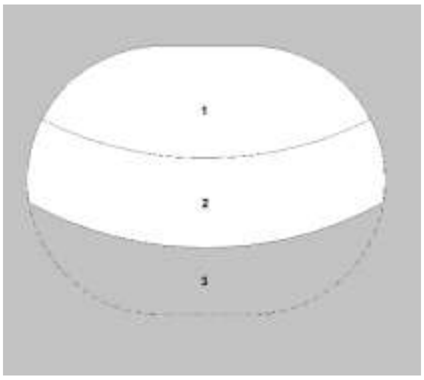

Figure 25. Construction stages of the section used in "Model 2"

CONCLUSIONS

In this study, three tunnel sections were investigated and compared to illustrate the effect of shape on the soil deformations and straining actions with the aim at optimizing the tunnel excavation sequences in Egyptian soil conditions. Results of plane-strain finite elements numerical simulations showed that using different construction sequences of advancing the tunnel sections affect the soil behavior, and the optimized type of sequence is dependent on the soil properties and shape dimension of the tunneling section.

Results of the study showed that dividing tunnel section into small parts enabled to control plastic points and soil deformations. Moreover, in case of group one, which has a section with equal width and height crown and bench excavations sequences are preferred for the sandy soil group; however, for the same group in clayey soil, side wall drift excavations sequences are preferred. In case of group two, which has a section with width smaller than its height, crown and bench excavation sequences are preferred in both sandy and clayey soil. In case of group three, which has a section with width larger than its height, side wall drift excavation sequences are preferred for both sandy and clayey soil groups. In case of large deformations, the crown and bench excavation sequence may be combined with side wall drift excavation sequence to reduce the surface settlements and, therefore, avoid any damages to the nearby structures or to avoid the ground from collapsing around the tunnel.

This study was done for underground opening at an average depth of 15 m in Cairo metro lines. In shallower depth, more investigations are needed. Dewatering and effect of ground water on underground opening should also be investigated. A further optimization concerning time-cost relationship in underground opening should be more studied.

REFERENCES

Thomas, A. 2019. Sprayed Concrete Lined Tunnels – 2nd ed. Abingdon, UK: Taylor & Francis. p. 288.

Arshad, R.A. Abdullah, A. 2016. A Review on Selection of Tunneling Method and Parameters Effecting Ground Settlement. Electronic Journal of Geotechnical Engineering.21(14): 4459-4462.

Eid, M.A. and M. Zaki AbdElrehim, M. Z. 2013. Optimization of Tunnel Profile in Different Ground Conditions Using Genetic Algorithms, 3rd International Conference on Computational Methods in Tunneling and Subsurface Engineering, Ruhr University Bochum.

FHWA. 2009. Technical Manual for Design and Construction of Road Tunnels – Civil Elements. U.S Department of Transportation Federal Highway Administration, publication No. FHWA-NHI-10-034, Washington, U.S.

Karakus M., Fowell R. J. 2004. An insight into the New Austrian Tunneling Method (NATM). Regional Rock Mechanics Symposium, Sivas, Turkey. p. 14.

Karakus M., Fowell R. J. 2003. Effects of different tunnel face advance excavation on the settlement by FEM. Tunneling and underground Tecknology, Vol. 18, Issue 5, p. 513-523.

L.C Vydrova. 2015. Comparison of tunneling methods NATM and Adeco RS.

Mahdi M., Shariatmadari N. 2014. Construction Procedures Evaluation of Three Adjacent Tunnels and Excavation Step Effects. World Academy of Science, Engineering and Technology, International Journal of Civil, Environmental, Structural, Construction and Architectural Engineering.8(1): 86-90.

MIDAS, MIDAS GTS NX V3.0.0(4). MIDAS GTS Manual, MIDAS Information Technology Co., Ltd, Gyeonggi 463-400, Korea.

Mostafa Z., Ahmed T. 2016. Effects of using Concrete Pre-Supporting Systems with NATM in construction of underground station, Journal of engineering Research.4(1): 1-20.

National Authority for Tunnels NAT. 2009. Greater Cairo Metro Report. Cairo, Egypt.

National Authority for Tunnels NAT. 2011. Geotechnical Interpretative Report, Haroun Station. Cairo, Egypt.

Rabcewicz, L.V. 1964 and 1965. The New Austrian Tunneling Method. Water Power, Part I, Vol. 16, 1964, pages 453-457 and Part III, Vol. 17, 1965, p. 19-24.

Said, Rushdie. 1962. The Geology of Egypt, Elsevier Pub. Co. New York, U.S., P.1-100/377.

Sauer, G. 1990. Design Concept for Large Underground Opening In Soft Ground Using The NATM. International Symposium on Unique Underground Structures, Denver, Colorado, Herndon, VA, USA.

Shata A.A. 1988. Geology of Cairo, Egypt. Volume 25, Issue 2 of Bulletin of the Association of Engineering Geologists.25(2): 149-183.